PHYSICAL REVIEW A VOLUME 39, NUMBER 12 JUNE 15, 1989

Collisional relaxation in an extended-pulse photon echo: Weak-field limit

Ru-wang Sung* and Paul R. Berman
Department of Physics, New York University, New York, New York 10003
(Received 27 July 1988)

The effect of velocity-changing collisions in an extended-pulse photon echo is studied. In an extended-pulse photon echo, the second excitation pulse has a duration comparable with the relaxation time of an atomic system. We present an analytic solution of the quantum-mechanical transport equation in the perturbation-theory limit and apply it to the extended pulse photon echo. It is found that the decay rate of the echo signal due to velocity-changing collisions is significantly modified by the variation of the second pulse's duration. The results are compared with those of conventional theories of two- and three-pulse echoes using temporally narrow excitation pulses. A physical interpretation of the results is given using both time- and frequency-domain arguments.

I. INTRODUCTION

It is well known that the photon echo represents a nonlinear laser spectroscopic technique which has been widely used for Doppler-free measurements since it was first discovered in the optical domain in 1964.[1] Photon-echo experiments were found to be very useful for studying velocity-changing collisions, owing to the fact that the photon-echo signal is Doppler free and that phase information associated with the velocity of atoms is preserved in the whole process. Many experiments[2-11] have demonstrated that the photon echo can serve as a highly sensitive probe of the various population and coherence collision kernels that characterize an atomic vapor. For example, consider a photon-echo experiment performed in a vapor, in which the two excitation pulses applied are separated by a time T and the echo is produced at time $2T$. The durations of the pulses are shorter than all relevant inverse frequencies in the problem. We refer to such a short-duration pulse excitation scheme as a *conventional photon echo* (CPE). The active atoms interact with the external fields and undergo collisions with perturber atoms in the medium. If collisions are phase interrupting in their effect on the electric-dipole coherence, the signal decays with a simple exponential form whose exponent is proportional to the pulse separation, whereas if they are velocity changing in nature, the exponent is a more complicated function of the pulse separation.[3]

A theory of the photon echo in the presence of velocity-changing collisions was given previously based on a quantum-mechanical transport equation (abbreviated as QMTE).[12-18] To be able to apply the QMTE to the photon-echo problem, it is required that the system be subject to certain physical assumptions and approximations. One assumption is that the duration of a collision is smaller than any time scale in the problem, which provides the validity of the binary collision and impact approximations. For the CPE, with certain collision kernels, an analytic solution of a simplified QMTE (neglecting the relaxation during short excitation pulses) can be obtained, which predicts the relative echo amplitude as a function of pulse separation. The situation changes if one or both of the excitation pulses is of a longer duration, such that relaxation effects can no longer be neglected during the pulses. Both the atom-field and collisional interactions need to be taken into account in the same time interval. Specifically, if the first pulse is narrow and the second pulse is comparatively very long, which we refer to as an *extended-pulse photon echo* (EPPE), the QMTE applied to the long-pulse interval leads to a set of coupled differentio-integral equations which are difficult to solve. For weak radiation fields, however, a perturbation approach can be used to solve the QMTE. For strong fields, a general solution of the QMTE for an extended pulse has not been found, to our knowledge. Experimentally, Yodh and co-workers[19] carried out an extended-pulse photon experiment using Yb vapor. In that experiment, they observed that the signal decay rate is affected dramatically by the duration of the second pulse when it is made sufficiently long. They explained their result on the basis of a strong-field quenching of collisional effects. To examine this hypothesis in greater detail, one must solve the QMTE in the presence of velocity-changing collisions for a strong field having arbitrary duration. We will discuss an analytic method for solving the QMTE in the strong-field limit in a subsequent paper.

In this work, we present a perturbative solution for the EPPE that illustrates some of the underlying physical principles and serves as a background for the strong-field calculation. The extended-pulse echo scheme can serve as a prototype problem in which the combined effects of strong fields and velocity-changing collisions act on electric-dipole coherence. Since velocity changes correspond, in effect, to a change in the atomic resonance frequency as viewed in the laboratory frame, the relaxation mechanism is representative of a perturbation that results in jumps of the transition frequency.

The purpose of the present work is to study the effect of velocity-changing collisions under an extended weak pulse by solving the QMTE from a perturbative approach. In order to gain physical insight into collisional effects in EPPE, it is very important to first analyze sys-

tematically the dephasing-rephasing processes experienced by atomic dipoles for no velocity-changing collisions. The dephasing-rephasing processes in EPPE is more complicated than it is in CPE and the corresponding phase diagrams exhibit some features analogous to those associated with conventional stimulated photon echoes (SPE) involving three excitation pulses of short duration.[16] Consequently it will prove useful to review the manner in which each velocity subclass contributes to echo formation in both CPE and SPE. Following the discussion of echo formation in the absence of collisions, we include the effects of velocity-changing collisions and solve the EPPE problem using a perturbative approach to treat the atom-extended field interaction. Based on the result, one will be able to see that the phase shift induced by velocity-changing collisions depends critically on the duration of the second pulse, leading to a significant modification of the signal decay rate.

The paper is organized as follows. In Sec. II, we consider the problem in the absence of velocity-changing collisions. The basic theory and equations are reviewed for analyzing the dephasing-rephasing processes in echo formation, including homogeneous relaxation produced by spontaneous emission or phase-interrupting collisions. A comparison is made between short-pulse and extended-pulse echoes. In Sec. III, we examine the effect of velocity-changing collisions for both short-pulse and extended-pulse photon echoes. A perturbation solution of the QMTE and its application to EPPE is presented for a so-called weak-collision kernel. Finally, we give a physical interpretation of this solution and compare it with those of CPE and SPE.

II. ECHO FORMATION AND RELAXATION: NEGLECT OF VELOCITY-CHANGING COLLISIONS

To account for photon-echo formation and relaxation using various excitation schemes, we discuss (Sec. II A) the basic theory, (Sec. II B) the dephasing-rephasing process in short-pulse and extended-pulse echo formation, and (Sec. II C) the modification of echoes due to spontaneous emission or phase-interrupting collisions.

A. Basic theory and equations

The photon-echo signal represents radiation emitted as a result of a macroscopic polarization created in an ensemble of atoms following interaction with a laser field. The atoms are assumed to consist of nondegenerate two-level atoms with upper state 2 and lower state 1 separated by frequency ω (see Fig. 1). The spatial and temporal variation of the echo-field amplitude $E_e(Z,t)$ and the polarization $P(Z,t)$ are related through the wave equation[20]

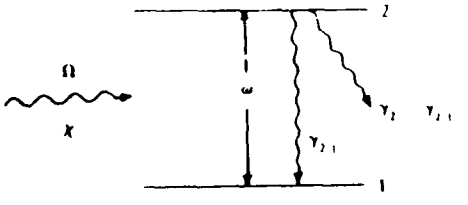

FIG. 1. Two-level quantum system considered in this work.

$$\frac{\partial^2 E_e(Z,t)}{\partial Z^2} - \frac{1}{c^2}\frac{\partial^2 E_e(Z,t)}{\partial t^2} = \frac{4\pi}{c^2}\frac{\partial^2 P(Z,t)}{\partial Z^2} , \tag{2.1}$$

where we have assumed that the laser field is polarized in the X direction and propagates in the Z direction, i.e.,

$$\mathbf{E}_L(Z,t) = \hat{\mathbf{X}} E_0(t)\cos(kZ - \Omega t) . \tag{2.2}$$

The field has propagation vector $\mathbf{k} = (\Omega/c)\hat{\mathbf{Z}}$, frequency Ω which is taken to be resonant with the atomic transition frequency ω, and amplitude $E_0(t)$ which, in general, is a slowly varying function of t compared with $\cos(\Omega t)$. To calculate the echo-field amplitude $E_e(Z,t)$, one must calculate the induced polarization $P(Z,t)$ which is related to the off-diagonal density-matrix element ρ_{12} (or ρ_{21}) associated with the ensemble of two-level atoms.

Neglecting velocity-changing collisions, but including the effects of spontaneous emission and phase-interrupting collisions, one has the standard equations for the time evolution of density-matrix elements given by

$$\dot{\rho}_{11}(v,t) = -\gamma_1\rho_{11}(v,t) + \gamma_{2,1}\rho_{22}(v,t) - i\chi(t)[\rho_{12}(v,t) - \rho_{21}(v,t)] , \tag{2.3a}$$

$$\dot{\rho}_{22}(v,t) = -\gamma_2\rho_{22}(v,t) + i\chi(t)[\rho_{12}(v,t) - \rho_{21}(v,t)] , \tag{2.3b}$$

$$\dot{\rho}_{12}(v,t) = -(\gamma_{12} + \Gamma_{ph} - ikv)\rho_{12}(v,t) - i\chi(t)[\rho_{11}(v,t) - \rho_{22}(v,t)] , \tag{2.3c}$$

$$\dot{\rho}_{21}(v,t) = -(\gamma_{12} + \Gamma_{ph} + ikv)\rho_{21}(v,t) + i\chi(t)[\rho_{11}(v,t) - \rho_{22}(v,t)] , \tag{2.3d}$$

where $\chi(t) = \mu_{12}E_0(t)/2\hbar$ is a Rabi frequency (μ_{12} is a dipole matrix element), $\gamma_i (i = 1,2)$ is the spontaneous emission rate of level i, $\gamma_{2,1}$ is the spontaneous emission rate from 2 to level 1, $\gamma_{12} = (\gamma_1 + \gamma_2)/2$, Γ_{ph} is a phase-interrupting collision rate, and v is the z component of the atomic velocity. The primary task is to evaluate the time-dependent density-matrix elements when atoms are subjected to different excitation schemes.

B. Echo formation neglecting relaxation

We solve Eq. (2.3), in which all spontaneous emission rates are set to zero, to predict the occurrence time of echoes and to see how the echo amplitude varies with pulse duration. Although the calculation and the interpretation of results of CPE and SPE is straightforward, we review it for completeness and for comparison with that of EPPE.

1. Short-duration pulses: CPE and SPE

It should be pointed out that, in many short-duration pulse echo experiments, the pulse areas defined by $2\chi T_p$ (Rabi frequency times a pulse duration) are taken to be $\pi/2$ and π, implying that the field strength is strong if the pulse is short. A perturbation theory requiring $\chi T_p \ll 1$ is not applicable for this case. Although Eq. (2.3) can be solved exactly for arbitrary field strength if decay is

neglected, for overall consistency with our calculation, we maintain a weak-field limit, assuming the pulse area is much less than unity. A symbol t^- or t' is used in the following calculations to denote the times right before or after an short excitation pulse occurring at time t.

In CPE, two light pulses (1 and 2), separated by a time interval T, are collinearly incident on an atomic sample. The pulse duration T_{pj} ($j=1,2$, for pulses 1 and 2) is assumed to be much shorter than the inhomogeneous dephasing time $1/ku$ so that the field can interact with all velocity subclasses simultaneously (u is the most probable speed of the active atoms). The corresponding diagram of this excitation pulse sequence is shown in Fig. 2. For $t > T'$, a perturbation solution of Eqs. (2.3) leads to a density-matrix element $\rho_{21}(v,t)$ responsible for echo formation given by

$$\rho_{21}(v,t) = -i\chi_1\chi_2^2 T_{p1}T_{p2}^2 e^{-ikv(t-2T)}\rho_{11}(v,0) , \qquad (2.4)$$

where χ_j is the Rabi frequency for a field having amplitude E_j. At $t=2T$, the Doppler dephasing produced from 0 to T is canceled exactly by the rephasing produced from T to $2T$, and the photon echo signal is emitted. The occurrence time of the maximum of the echo signal is called the echo time and denoted by t_e in this paper. The dephasing-rephasing feature of this short-pulse echo is that atomic dipoles in each velocity subclass acquire their maximum absolute phase at the same time T; the field then reverses these phases simultaneously, and the dipoles all return to the initial phases at the same time $2T$. This feature is schematically shown in the phase diagram of Fig. 3

By carrying out the integration of Eq. (2.4) over the whole velocity range at $t=2T$, one finds that the off-diagonal density-matrix element contributing to the echo is

$$\rho_{21}(t_e) = -i\chi_1\chi_2^2 T_{p1}T_{p2}^2 . \qquad (2.5)$$

It is seen that the echo amplitude [proportional to $|\rho_{21}(t_e)|$] increases with the second pulse area as $(\chi_2 T_{p2})^2$ as long as the restrictions for the pulse width $kuT_{p2} \ll 1$ and $\chi_2 T_{p2} \ll 1$ hold. Physically, this result reflects the fact that the second pulse first creates a population difference which the field then acts upon to create stimulated emission associated with the coherence density ρ_{21}. If the pulse duration is sufficiently short so that any Doppler dephasing during the pulse can be neglected, the amplitude for each step in this excitation is proportional to the pulse area $\chi_2 T_{p2}$ so that the final echo amplitude

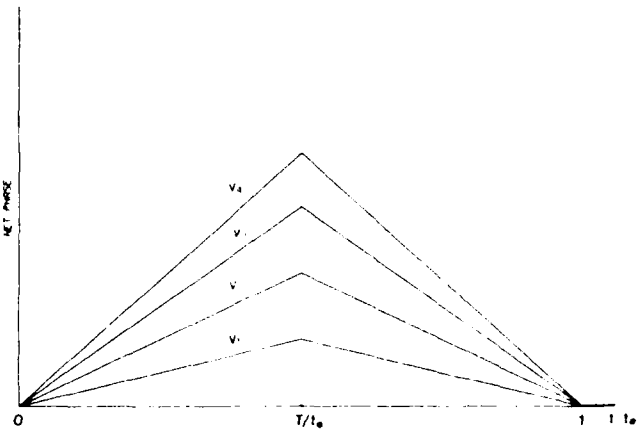

FIG. 3 Phase diagram associated with four velocity subclasses of dipoles in CPE. The initial relative phase of the dipoles is zero. For $t>0$, the dipoles dephase relative to each other following the diagonal lines whose slopes are determined by the velocities of the dipoles. They all reach the maximum phase values at time T. Then the phases are reversed simultaneously and return to the initial value at time $t_e = 2T$.

depends quadratically on the pulse area of the second field.

In order to lay the groundwork for an understanding of the dephasing-rephasing processes in an extended-pulse photon echo, it is useful at this time to also review the formation of a stimulated photon echo. The SPE is produced by three short excitation pulses as shown in Fig. 4. Pulses 1 and 2 are separated by time T_1 and pulses 2 and 3 by time $T_2 - T_1$. The pulse durations T_{pj} ($j=1,2,3$) satisfy the same conditions as those in CPE, i.e., they are much shorter than $1/ku$ and $1/\chi$. A perturbation calculation leads to a contribution to $\rho_{21}(v,t)(t > T_2)$ responsible for SPE given by

$$\rho_{21}(v,t) = -2i\chi_1\chi_2\chi_3 T_{p1}T_{p2}T_{p3} e^{-ikv(t-T_2+T_1)}\rho_{11}(v,0) . \qquad (2.6)$$

Consequently, one finds that the echo occurs at $t_e = T_2 + T_1$ when the phase kvT_1 buildup between pulses 1 and 2 is totally canceled by the phase $[-kv(t-T_2)]$ developed between pulse 3 and the echo time. It is useful to redefine the echo time as $t_e = 2t_c$, where t_c denotes the central time between pulse 2 and pulse 3 given by $t_c = (T_1 + T_2)/2$ which reflects a symmetry property that

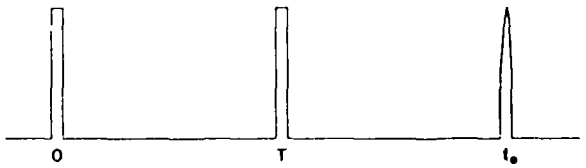

FIG. 2. Excitation pulse sequence of conventional two-pulse photon echo (CPE). The echo is emitted at $t_e = 2T$.

FIG. 4. Excitation pulse sequence of conventional three-pulse photon echo (SPE). The echo is emitted at $t_e = T_1 + T_2$.

A-1 21

will prove useful in analyzing the echo formation in EPPE. The phase diagram in Fig. 5 displays the dephasing-rephasing processes in SPE. The diagonal lines with different slopes represent the dephasing period associated with different velocity subclasses of atomic dipoles from 0 to T_1, the horizontal lines represent the constant phase period associated with atomic state populations from T_1 to T_2, and the diagonal lines with the opposite signs of slopes from T_2 to the echo time represent the rephasing period for the atomic dipoles.

We have reviewed the formation of photon echoes with two and three short pulses, respectively, and find that in the two-pulse case the echo occurs at $2T$ and in the three-pulse case the echo occurs at $T_2 + T_1 = 2t_c$. In both cases the maximum of the signal essentially occurs at the time when the different velocity subclasses of atomic dipoles have rephased relative to one another. The amplitude of the echo in the two-pulse case is found to increase with the second-pulse duration quadratically, provided a perturbation treatment and the inequality $kuT_{p2} \ll 1$ are valid. These results are to be compared with the extended-pulse echo case to be discussed below.

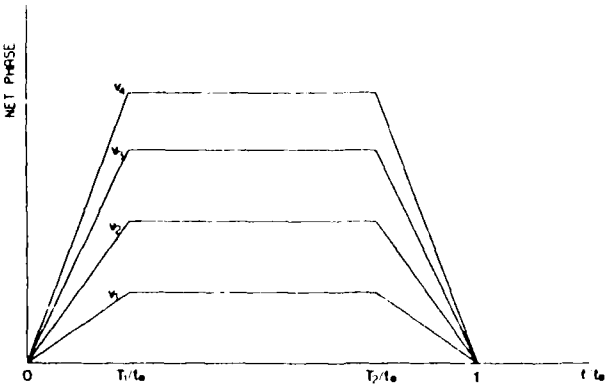

FIG. 5. Phase diagram associated with four velocity subclasses in SPE. The dephasing-rephasing processes associated with coherence in time intervals $0 \to T_1$ and $T_2 \to t_c$ are represented by diagonal lines. The phase preserved from T_1 to T_2 through population density is represented by horizontal lines.

2. *Extended-pulse photon echo: EPPE*

Two-level atoms subject to the excitation pulse scheme shown in Fig. 6 can produce a photon echo, in which the first field acts from 0 to t_1, the second field acts from t_2 to t_3, and the echo signal occurs at $t = t_3 + t_2 - t_1$. The dephasing-rephasing process in the whole period in this case is more complicated than in the conventional theory of short-pulse photon echoes because the dephasing-rephasing processes have to be taken into account during the atom-field interaction. In this section, we present a perturbation solution of Eq. (2.3) to obtain the density-matrix element $\rho_{21}(t_c)$ (and, consequently, the echo amplitude) and see how it varies with the duration of the second pulse. A physical interpretation of the result using both time and frequency-domain arguments is given.

We assume that the first pulse remains of short duration satisfying the same condition as it does in CPE. The second pulse is extended to be longer than the inhomogeneous dephasing time $1/ku$, but is still shorter than the field-induced transition time $1/\gamma$ so that the perturbation calculation is still applicable. The perturbation calculation is still straightforward and one finds

$$\rho_{21}(t_c) = -2i\gamma_1\gamma_2^2 T_{p1}\int dv \int_0^{T_{p2}} d\tau' \int_0^{\tau'} d\tau'' e^{-(kv+\Delta)(T_{p2}-\tau'+\tau'')} \rho_{11}(v,0) . \tag{2.7}$$

We are interested in finding the time at which the maximum signal occurs and how its amplitude varies with the pulse duration. The discussion is based on the order in which the integration of Eq. (2.7) is performed.

Suppose one first carries out the velocity integration in Eq. (2.7) to obtain

$$\rho_{21}(t_c) = -2i\gamma_1\gamma_2^2 T_{p1}\int_0^{T_{p2}} d\tau' \int_0^{\tau'} d\tau'' e^{-[(ku/2)(T_{p2}-\tau'+\tau'')+\Delta](\tau'-\tau'')} . \tag{2.8}$$

The variables τ'' and τ' take on all values from zero to the length of pulse 2. However, the main contribution to the signal originates from those times satisfying the relation

$$|T_{p2} - \tau'' - \tau'| < \frac{2}{ku} , \tag{2.9a}$$

beyond which the signal falls off exponentially. This result can be interpreted in terms of conventional stimulated photon echoes. Condition (2.9a) can be rewritten as

$$|(t - t') - t''| \leq \frac{2}{ku} , \tag{2.9b}$$

where $t'' = \tau'' + t_2$ and $t' = \tau' + t_2$ are the interaction times for the second pulse relative to a time origin chosen at $t = 0$. In other words, if the interaction times are such that the Doppler phase accumulated in the period $0 \to t''$ is approximately canceled by the Doppler phase accumulated in the period $t' \to t$, there is a maximum contribution to the echo signal. This result is identical to that for a short-duration-pulse stimulated echo with interaction times $t_1 = 0$, $t_2 = t''$, $t_3 = t'$, as may be seen in Fig. 7. The second pulse is broken down into a sequence of strips and, owing to condition (2.9b), it is only those strips which are symmetrically located about the center of pulse 2 which contribute. Four such pulse pairs labeled aa', bb', cc', and dd' are shown in diagram (c) of Fig. 7. Each pair plus the first pulse constitutes a pulse sequence

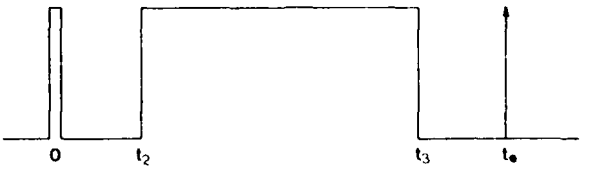

FIG. 6. Excitation pulse sequence of extended-pulse photon echo (EPPE). The maximum echo signal occurs at $t_e = t_3 + t_2 - t_1$, denoted by the arrow.

equivalent to that for a stimulated photon echo. The total contribution to the echo signal from the extended pulse is just the statistical summation of all the independent symmetric stimulated echoes. The inequality (2.9b) guarantees that each pulse pair accomplishes an exact phase cancellation by itself. If any asymmetric pulse pair were chosen, it would not contribute as significantly since the rephasing period from the second strip to the echo time is longer than the dephasing period from time zero to the first strip. From this time-domain result, one can note the following: (1) As in the conventional stimulated echo, *all velocity subclasses contribute equally* to the echo signal, and (2) of all the possible t'', t' pairs which could contribute to the echo signal, those pairs satisfying condition (2.9b) contribute most significantly. As is shown below, collisions further reduce the atom's interaction with the second excitation pulse.

An alternative way to analyze the echo formation with an extended pulse is to perform the time integration of Eq. (2.7) first to get an expression for the density-matrix element in the frequency (velocity) domain. The solution is

$$\rho_{21}(t) = -i\frac{\gamma_1\gamma_2^2 T_{p1}}{\sqrt{\pi}ku}\int_{-\infty}^{+\infty} e^{ik\nu(t-t_3+t_2)}\frac{\sin^2(k\nu T_{p2}/2)}{(k\nu/2)^2} \times e^{-(\nu/u)^2}d(k\nu)\,. \quad (2.10)$$

Figure 8 is a phase diagram associated with a single velocity subclass, showing all dephasing-rephasing possibilities. This figure differs from what we have seen in the short-pulse echo case in which atoms with the same velocity follow the same dephasing-rephasing path. In the EPPE, switching can occur at different times during the second pulse. By taking into account the contribution from all possible dephasing-rephasing paths corresponding to different switching times, one is lead to an oscillating function that varies as $\sin^2(k\nu T_{p2}/2)$. This factor itself does not provide any information for determining the echo time. By differentiating Eq. (2.10), however, one finds that the maximum echo signal occurs when $t - t_3 = t_2$. Physically, it predicts that the echo still occurs at the time when phase buildup in the interval $0 \to t_2$ is canceled by that built up in $t_3 \to t_e$ and the echo time is not affected by dephasing-rephasing processes during the second pulse. In this picture of echo forma-

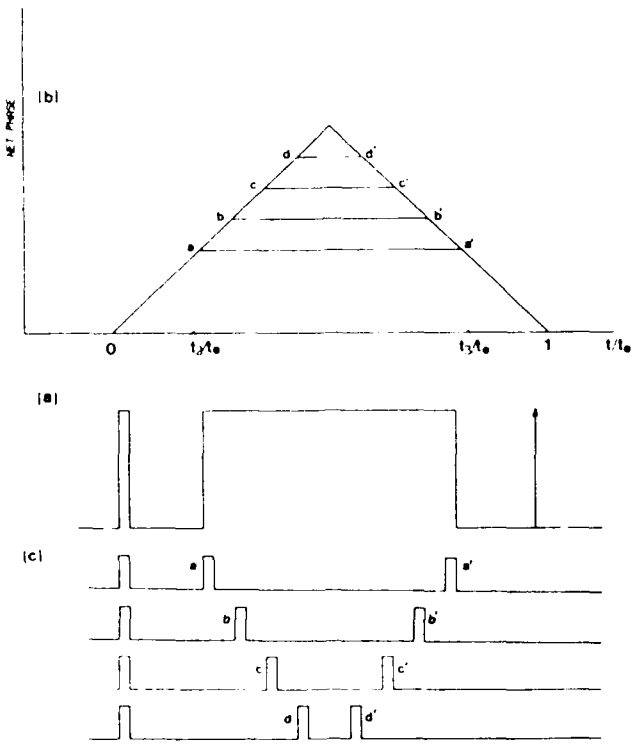

FIG. 7. Schematic representation of dephasing rephasing of atomic dipoles in the extended-pulse photon echo with the excitation pulse sequence shown in (a) and the phase diagram shown in (b). The phase diagram illustrates four symmetric phase paths associated with one velocity subclass of dipoles. Positions marked *aa'*, *bb'*, *cc'*, and *dd'* correspond to four groups of symmetric switching times during the second excitation pulse. Each phase path (for example, 0*aa'*1) can be viewed as arising from a corresponding short-duration-pulse stimulated echo in which the second and third excitation pulses are located symmetrically about $t = (t_3 + t_2)/2$. Four such sets of excitation pulse sequence are shown in (c). The extended-pulse photon echo in the weak-field limit can be interpreted as arising from a series of such symmetric stimulated photon echoes.

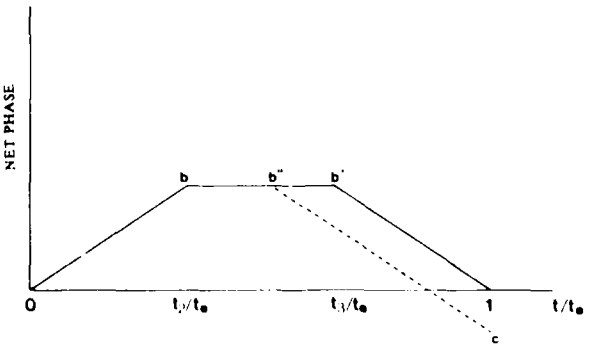

FIG. 8. Phase diagram associated with one velocity subclass of atomic dipoles in the EPPE. The description for the symmetric path (0*bb'*1) is the same as that in Fig. 7(b), which produces zero net phase at the time t_e. The asymmetric one (0*bb''*c) in which the first switching time is still at the time corresponding to the position *b* and the second switching time is asymmetrically located at the time corresponding to *b''* produces net phase (indicated by c) at the time t_e. Therefore, the extended-pulse photon echo results mainly from the dipoles which experience symmetric dephasing-rephasing processes.

tion, both the symmetric and asymmetric pulse excitation strips contribute; the "extra" phase produced at the echo time is reflected by the squared sinusoidal function. In the frequency domain, we find that different velocity subclasses do *not* contribute equally, with atoms having $kvT_{p2} \ll 1$ producing the major contribution to the signal. Slow atoms contribute more than fast atoms since the net Doppler phase for the slow atoms is less than that for the fast ones (see Fig. 9).

The interpretation of echo formation seems to depend on the order of integration. In the time domain, it seems that all velocity classes of atoms contribute to the echo signal, but only time strips symmetric about the center of the second pulse play a significant role. In the frequency domain, it seems that all time strips contribute, but that only slow atoms contribute significantly. In reality, neither of the above interpretations is strictly true owing to the finite (rather than infinite) width of the atomic velocity distribution. The numerical calculations indicate that the major contribution arises from symmetric time strips in pulse 2 and from slowly moving atoms.

The discussion based on both the time and the frequency domains is helpful for understanding the formation of echoes with an extended pulse and will help us to analyze the effects of velocity-changing collisions on dephasing-rephasing processes. By carrying out the velocity integration of Eq. (2.10), one can obtain the echo amplitude. The numerically integrated result of $\rho_{21}(t_e)$ is plotted in Fig. 10. In the limit that $kuT_{p2} \gg 1$, one finds

$$\rho_{21}(t_e) \approx \frac{4\pi\bar{\nu}\gamma_1\gamma_2^2 T_{p1}T_{p2}}{ku} . \tag{2.11}$$

It is seen that the echo amplitude with an extended pulse

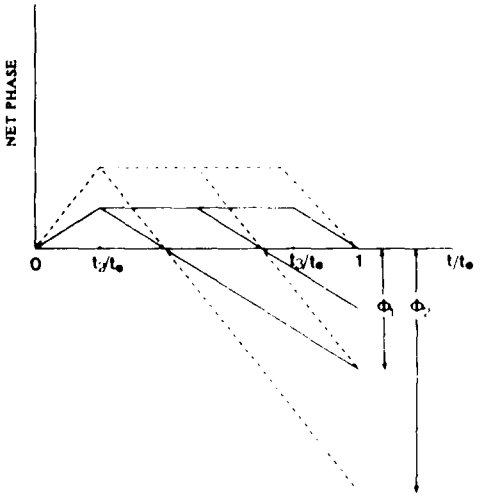

FIG. 9. Phase diagram associated with two velocity subclasses of dipoles in the EPPE. The solid and dashed lines represent several possible symmetric and asymmetric phase paths for atoms having velocities v_1 and v_2, respectively. At the time t_e, the range of net phases produced by the asymmetric phase paths are denoted by Φ_1 and Φ_2 for v_1 and v_2, respectively. Note that $\Phi_2 \gg \Phi_1$, since $v_2 \ll v_1$. This illustration supports a frequency-domain argument in which the slow atoms contribute the major part to the extended-pulse photon echo.

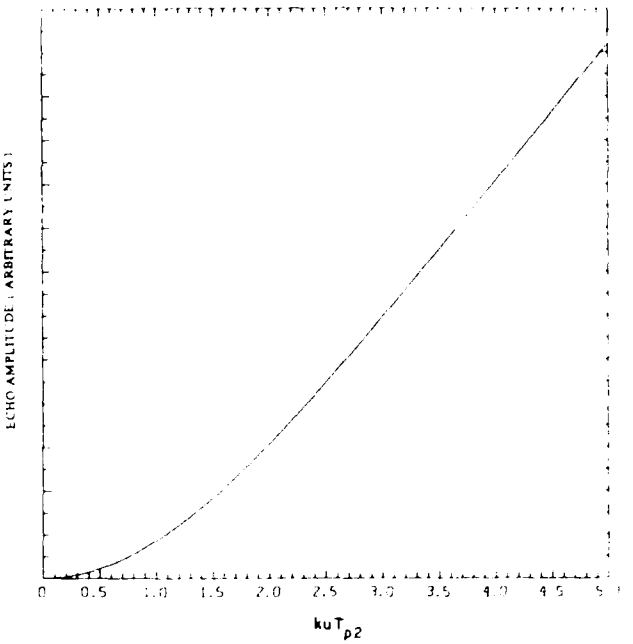

FIG. 10. Variation of the photon-echo amplitude with the second pulse's duration T_{p2} in the absence of relaxation effects. This approach represents a numerical solution to Eq. (2.10). For $kuT_{p2} \ll 1$, the echo amplitude increases quadratically with T_{p2}, while for $kuT_{p2} \gg 1$, the echo amplitude increases linearly with T_{p2}.

increases linearly with the second-pulse duration T_{p2} (once $kuT_{p2} \gg 1$) rather than quadratically as in the short-pulse case. It is very convenient to interpret this result in the time domain. As discussed above, the contribution of a long second pulse to the echo comes from many symmetrical short pulses equivalent to an SPE. The amplitude of each SPE is proportional to the product of its three excitation pulse widths. According to the relation of Eq. (2.9a), each symmetric pulse within pulse 2 has an effective width of $1/ku$. The amplitude of each SPE is then proportional to $T_{p1}(1/ku)(1/ku)$. The number of pulse pairs are $T_{p2}/(1/ku)$. By summing over all contributions, one finds the amplitude of the extended-pulse echo is proportional to

$$T_{p1}\frac{1}{(ku)^2}\frac{T_{p2}}{(1/ku)}$$

which agrees with Eq. (2.11).

One can also understand the form of the echo signal by considering the manner in which the second pulse creates population and coherence. For a short pulse, there is no dephasing among the dipoles being considered during the time in which the field acts and the increase of the pulse area yields the net effect of creating a larger population difference (proportional to $\gamma_2 T_{p2}$) as well as stimulating more dipoles to emit (also proportional to $\gamma_2 T_{p2}$), so that the echo amplitude varies as the square of the second pulse area $(\gamma_2 T_p)^2$. For a long pulse the dipoles dephase in a time of order $1/ku$. If $T_{p2} \gg 1/ku$ the effective coherence density created by the second field is propor-

tional to $\chi_2(1/ku)$ because the second pulse length is reduced to an effective time $1/ku$ as far as the coherence density is concerned. The population density will still increase as $\chi_2 T_{p2}$ since phase interference is not related to the creation of population density. These two factors lead to a contribution to the echo amplitude that varies with the second pulse as $\chi_2^2 T_{p2}/ku$.

It should be pointed out that we have calculated ρ_{21} at $t=t_e$, the time at which the peak of the echo signal occurs. The actual signal extends over a time interval equal to T_{p2}. Moreover, there is also a "nonecho" contribution to the signal at $t=t_e$, arising from free-induction decay following the second pulse. Thus, there are complications involved in experimentally measuring a quantity which corresponds to the echo-field amplitude. We defer a discussion of this question to the following paper.

C. Inclusion of relaxation

The photon-echo signal decays as a result of various relaxation mechanisms such as spontaneous emission and phase-interrupting collisions (velocity-changing collisions are neglected in this section). We use Eqs. (2.3) and choose a relaxation scheme in which there is no population loss, i.e., $\gamma_1=0$, $\gamma_{2,1}=\gamma_2$, to examine the modification of photon echoes produced by spontaneous emission and phase-interrupting collisions for the short-duration pulse and the extended-pulse case, respectively.

1. Short-duration pulses: CPE and SPE

In CPE, relaxation in the excitation regions is neglected. One can easily solve Eqs. (2.3) to find that the echo decays exponentially as

$$\rho_{21}(t_e)=-i\chi_1\chi_2^2 T_{p1}T_{p2}^2 e^{-2(\gamma_{12}+\Gamma_{ph})T} . \tag{2.12}$$

In SPE, relaxation is also neglected in the pulse regions. By solving Eqs. (2.3) for the various time regions, one obtains

$$\rho_{21}(t_e)=-2i\chi_1\chi_2\chi_3 T_{p1}T_{p2}T_{p3} \times e^{-(\gamma_{12}+\gamma_{ph})[t_e-(T_2-T_1)]-\gamma_2(T_2-T_1)} . \tag{2.13}$$

The physical interpretation of this result is straightforward. The term $e^{-(\Gamma_{ph}+\gamma_{12})[t_e-(T_2-T_1)]}$ represents the decay of coherence density occurring in intervals T_1 and t_e-T_2, and the term $e^{-\gamma_2(T_2-T_1)}$ represents the decay of population density occurring in the second pulse interval in which there is no collision-induced decay.

2. Extended pulse: EPPE

These results can now be taken over to analyze the effects of relaxation in the extended-pulse echo.[21] By solving Eqs. (2.3) with $\gamma_1=0$ and $\gamma_{12}=\gamma_2/2$, one can find a coherence density

$$\rho_{21}(t_e)=\frac{-2i\sqrt{\pi}\chi_1\chi_2^2 t_1}{ku(\Gamma_{ph}-\gamma_{12})}e^{-(\Gamma_{ph}+\gamma_2/2)t_e} \times(e^{(\Gamma_{ph}-\gamma_2/2)T_{p2}}-1) . \tag{2.14}$$

In two special limiting cases, i.e., $\gamma_2 t_e \ll 1$ or $\Gamma_{ph}=0$, we have

$$\rho_{21}(t_e)=\frac{-2i\sqrt{\pi}\chi_1\chi_2^2 t_1}{ku}e^{-\Gamma_{ph}(t_e-T_{p2})} \times\left|\frac{1-e^{-\Gamma_{ph}T_{p2}}}{\Gamma_{ph}}\right| \quad \text{for } \gamma_2 t_e \ll 1 \tag{2.15a}$$

and

$$\rho_{21}(t_e)=\frac{-4i\sqrt{\pi}\chi_1\chi_2^2 t_1}{ku}e^{-\gamma_{12}(t_e-T_{p2})} \times\left|\frac{e^{-(\gamma_2/2)T_{p2}}-e^{-\gamma_2 T_{p2}}}{\gamma_2}\right| \quad \text{for } \Gamma_{ph}=0 . \tag{2.15b}$$

We can compare Eqs. (2.15a) and (2.15b) with Eq. (2.11) for the extended-pulse photon echo without relaxation and Eq. (2.13) for the conventional stimulated echo. (a) For $\gamma_2 t_e \ll 1$ and Γ_{ph} arbitrary, the factor $1/ku$ remains in the EPPE (2.15a) because Doppler dephasing still exists. The signal decays exponentially during intervals (t_2-t_1) and (t_e-t_3), owing to phase-interrupting collision, leading to the exponent $\Gamma_{ph}[(t_2-t_1)+(t_e-t_3)]=\Gamma_{ph}(t_e-T_{p2})$ in Eq. (2.15a). During the second excitation pulse, the atom still decays as a result of phase-interrupting collisions before it is switched into a population density. By taking an average over excitation times, one finds that the signal decays in the second pulse interval as $(1-e^{-\Gamma_{ph}T_{p2}})/\Gamma_{ph}$. Since phase-interrupting collisions are associated with coherence density only, atoms that are switched into population during pulse 2 no longer experience collisional dephasing; consequently, the relaxation produced by phase-interrupting collisions is reduced during the second pulse. In comparison with the SPE, however, the decay due to collisions in the EPPE is not completely suppressed as in the SPE, because there is a range of "switching times" in EPPE rather than the single set of switching times encountered in CPE. (b) For $\Gamma_{ph}=0$ and $\gamma_2 t_e$ arbitrary, the signal decays at rate γ_{12} in two intervals: t_2-t_1 and t_e-t_3. In the long-pulse region, the coherence decays at rate γ_{12} and population decays at rate γ_2. Since atoms are switched into population density at different times, one obtains the modified decay form given by (2.15b). In the SPE, the decay between pulses 2 and 3 represents population decay from level 2 to 1 as $e^{-\gamma_2 T_{p2}}$; in the EPPE, the result represents the combined effect of decay for coherence and population during the second excitation pulse. These two limiting cases for SPE and EPPE will help us to understand the relaxation induced by velocity-changing collisions.

We conclude the discussion for CPE, SPE, and EPPE in the absence of velocity-changing collisions by noting the following. (1) The echo time is essentially determined by the pulse delay time in CPE, the central time between pulse 2 and pulse 3 in SPE, and the central time of the

second pulse in EPPE. It is influenced neither by the pulse duration in EPPE not by the separation time between pulse 2 and pulse 3 in SPE. (2) In the absence of relaxation, the echo amplitude increases quadratically with the second pulse's duration as long as $kuT_{p2} \ll 1$ in CPE and linearly with the pulse duration in EPPE, if $kuT_{p2} \gg 1$. (3) The formation of EPPE can be considered as arising from a summation of stimulated echoes in which the second and third "excitation pulses" are strips having duration $(ku)^{-1}$ that are symmetrically located about the center of the long-duration excitation pulse. Slow atoms $[kv < (1/T_{p2})]$ give the major contribution to echo formation. (4) With the inclusion of spontaneous emission and phase-interrupting collisions, the CPE signal decays exponentially at the rate $\gamma_{12} + \Gamma_{ph}$ over the entire period. From 0 to T_1 and from T_2 to t_e, the EPPE signal decays exponentially at the rate $\gamma_{12} + \Gamma_{ph}$ and the decay rate is modified in the region $T_2 - T_1$ in a manner that depends on both the population and coherence decay rates.

III. EFFECT OF VELOCITY-CHANGING COLLISIONS ON PHOTON ECHOES

In this section, we consider a vapor of active atoms and perturbers. The active atoms interact with the external light field and undergo collisions with perturber atoms. In order to analyze more clearly the effect of collisions on photon echoes, we suppress the contribution from spontaneous emission. The duration of a collision is assumed to be less than any of the relevant time scales in the problem so that collision-induced velocity changes can be viewed as an instantaneous process. This assumption allows one to make a binary collision and an impact approximation. Essentially, this collisional relaxation can be viewed as a Markovian process which characterizes the property of a stochastic process.[22,23] In general, a Markovian process represents one in which a distribution characterizing the system following a stochastic fluctuation (for example, a collision) depends, at most, on its value before the fluctuation. It is very convenient to use the Markovian approximation for modeling velocity-changing collision processes and it enables one to treat the effects of external fields and collisions independently. Implicit in the Markovian approximation is the assumption that the perturber reservoir is sufficiently large to be unaffected by active-atom-perturber collisions. It is also assumed that the active-atom density is low enough to neglect all active-atom–active-atom collisions. Thus, the collisional contribution to the rate of time change of the atoms' density-matrix elements can be written as[16]

$$\dot{\rho}_{ij}(v,t)|_{coll} = -(\Gamma_{ij}^{ph} + \Gamma_{ij})\rho_{ij}(v,t) + \int w_{ij}(v'-v)\rho_{ij}(v',t)dv' , \tag{3.1}$$

with

$$\Gamma_{ij} = \int w_{ij}(v'-v)dv' ,$$

where $\Gamma_{ij}^{ph}[=\Gamma_{ph}(1-\delta_{ij})]$ and Γ_{ij} are phase-interrupting and velocity-changing collision rates, respectively, and w_{ij} is a collision kernel that gives the probability density per unit time that a collision changes the velocity of an active atom associated with ρ_{ij} from v' to v.

To illustrate the physical principles, we choose a simple model[16] in which large-angle scattering results in a decay term of atomic coherence, and small-angle scattering results in equal collision kernels and rates for atomic state populations and coherence, i.e.,

$$\Gamma_{11} = \Gamma_{ij} = \Gamma , \qquad w_{11}(v'-v) = w_{ij}(v'-v) = w(v'-v) . \tag{3.2}$$

By adding Eq. (3.1) to Eqs. (2.3) in which we set $\gamma_2 = \gamma_{12} = 0$, we arrive at a simplified quantum-mechanical transport equation[16]

$$\dot{\rho}_{11}(v,t) = -i\chi[\rho_{12}(v,t) - \rho_{21}(v,t)] - \Gamma\rho_{11}(v,t) + \int w(v'-v)\rho_{11}(v',t)dv' , \tag{3.3a}$$

$$\dot{\rho}_{22}(v,t) = i\chi[\rho_{12}(v,t) - \rho_{21}(v,t)] - \Gamma\rho_{22}(v,t) + \int w(v-v)\rho_{22}(v',t)dv' , \tag{3.3b}$$

$$\dot{\rho}_{12}(v,t) = -(\Gamma + \Gamma_{ph} - ikv)\rho_{12}(v,t) - i\chi[\rho_{11}(v,t) - \rho_{22}(v,t)] + \int w(v'-v)\rho_{12}(v',t)dv' , \tag{3.3c}$$

$$\dot{\rho}_{21}(v,t) = -(\Gamma + \Gamma_{ph} + ikv)\rho_{21}(v,t) + i\chi[\rho_{11}(v,t) - \rho_{22}(v,t)] + \int w(v'-v)\rho_{21}(v',t)dv' . \tag{3.3d}$$

Notice that Eq. (3.3) contains collision kernels which depend solely on v_z' and v_z, although the z subscript does not appear explicitly. In effect, Eqs. (3.3) represent an approximate solution, since we neglect the collision-induced coupling of transverse and longitudinal velocity components.[16]

Since the functional dependence of the result is independent of the specific form of the collision kernel, we adopt a "difference" kernel[24]

$$w(v'-v) = \frac{\Gamma}{\sigma\sqrt{\pi}} e^{-[(v'-v)/\sigma]^2} \tag{3.4}$$

(recall that $\sigma/\sqrt{2}$ is the rms velocity jump per collision). Such a kernel does not obey detailed balance, but can be used successfully to model weak collisions (small-angle scattering). We solve Eq. (3.3) using a perturbative approach, and apply the results to CPE, SPE, and EPPE, respectively, to explore how collisions disturb the dephasing-rephasing processes and cause a decrease in echo amplitude.

A. Short-duration pulses: CPE and SPE

In CPE, the duration of the pulses is shorter than any time scales in the problem, i.e., $\Gamma_{ph}T_{pj} \ll 1$, $\Gamma T_{pj} \ll 1$, $\gamma_j T_{pj} \ll 1$, and $kuT_{pj} \ll 1$ $(j=1,2)$. After the first pulse, atomic dipoles are created. Between pulse 1 and 2, these dipoles dephase relative to each other and, at the same

time, undergo collisions with perturbers. Between pulse 2 and the echo, the dipoles rephase while also undergoing collisions with perturbers. For the kernel (3.4), the resultant signal can be calculated using Fourier transform (FT) techniques and one finds[3-5]

$$\rho_{21}(t_e)=-i\chi_1\chi_2^2 T_{p1}T_{p2}^2 \times\exp\left\{-\Gamma_{\rm ph}t_e-2\Gamma T\times\left[1-\frac{\sqrt{\pi}}{k\sigma T}\mathrm{erf}(k\sigma T/2)\right]\right\}, \tag{3.5}$$

where erf stands for the error function.

It is interesting to note that the echo signal decays exponentially in the whole interval at rate $\Gamma_{\rm ph}$ due to phase-interrupting collisions and at an effective rate

$$\Gamma[1-(\sqrt{\pi}/k\sigma T)\mathrm{erf}(k\sigma T/2)]$$

due to velocity-changing collisions. This effective rate is a measure of the degree of collisional interference with the Doppler dephasing-rephasing process of echo formation, and depends critically on the phase shift $k\sigma T$. When $k\sigma T \ll 1$, the phase shift in the whole interval is not large enough to modify the Doppler-phase cancellation, and velocity-changing collisions do not alter the echo signal

$$\exp\{-2\Gamma T[1-(\sqrt{\pi}/k\sigma T)\mathrm{erf}(k\sigma T/2)]\}\approx 1 .$$

On the other hand, if $k\sigma T>1$, any atom that collides experiences a large collision-induced phase fluctuation and one would expect an echo amplitude that decays as $\exp(-2\Gamma T)$, reflecting contributions from only those atoms that undergo no collisions in the time interval. Actually, this conclusion is only approximately correct. For atoms undergoing collisions in the time intervals $0<t<(k\sigma)^{-1}$ and $2T-(k\sigma)^{-1}<t<2T$, the net phase change is of order $\Gamma/k\sigma$ which is not necessarily fatal to

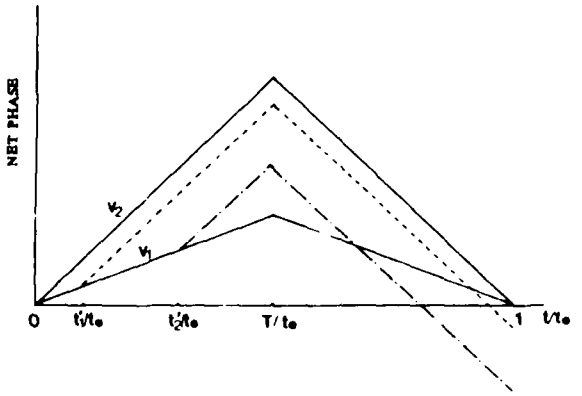

FIG. 11. Phase diagram associated with two velocity subclasses of dipoles with v_1 and v_2, showing the effect of velocity-changing collisions on echo formation in CPE. If a collision occurs at t_1', changing v_1 to v_2, after t_1', the dephasing-rephasing path follows the dashed line and a small phase shift at t_e is produced, which may not be fatal to echo formation. However, if the same type of collision occurs at t_2' then the phase shift at t_e is larger, which may destroy echo formation.

echo formation. As a consequence, the echo decays as

$$\exp\{-2\Gamma[T-(\sqrt{\pi}/k\sigma)]\}$$

instead of $\exp(-2\Gamma T)$, reflecting the fact that the effective time for collisional destruction is $2(T-\sqrt{\pi}/k\sigma)$ instead of $2T$. Figure 11 illustrates the effect of collisions, occurring at different times, on the echo signal.

Next, we explore the effect of velocity-changing collisions on the stimulated photon echo. Collisions occurring between pulses 1 and 2 and pulse 3 and the echo affect atomic state coherences, while those between pulses 2 and 3 modify atomic state populations. The resultant signal, again calculated by FT techniques, is found to be

$$\rho_{21}(t_e)=-2i\chi_1\chi_2\chi_3 T_{p1}T_{p2}T_{p3}e^{-2\Gamma_{\rm ph}T_1}\times\exp\left\{-2\Gamma T_1\left[1-\frac{\sqrt{\pi}}{k\sigma T_1}\mathrm{erf}(k\sigma T_1/2)\right]-\Gamma(T_2-T_1)\{1-\exp[-(k\sigma T_1)/2]^2\}\right\} . \tag{3.6}$$

One can note the following: (1) As was previously discussed, the decay induced by phase-interrupting collisions occurs only in the time intervals $0<t<T_1$ and $T_2<t<t_e$, which is associated with coherence densities. (2) The decay of the echo in the region $0<t<T_1$ and $T_2<t<t_e$, expressed by the first part of the exponential term in Eq. (3.6) is identical to that of CPE. (3) The modification of the decay rate in the region $T_1<t<T_2$, expressed by the second part of the exponential term in Eq. (3.6), indicates that the effect of velocity-changing collisions on population density strongly depends on the dephasing time T_1 as well as the number of collisions $\Gamma(T_2-T_1)$ occurring in the interval between pulse 2 and 3. Physically, this implies that if the dipole phase accumulated before the second pulse acts is sufficiently large, i.e., $k\sigma T_1 \gg 1$, collisions occurring in the interval $T_1<t<T_2$ significantly modify the phase. In this limit, only those atoms that have not collided in the time interval T_2-T_1 contribute to echo formation, and the signal varies as $\exp[-\Gamma(T_2-T_1)]$. For $k\sigma T_1 \ll 1$, collisions occurring in the region $T_1<t<T_2$ do not significantly modify the Doppler-phase factor, i.e., collisional decay of the echo signal is suppressed between T_1 and T_2. This result is expressed mathematically by the fact that

$$\exp(-\Gamma(T_2-T_1))\{1-\exp[-(k\sigma T_1)^2/2]^2\}\approx 1$$

when $k\sigma T_1 \ll 1$.

B. Extended-pulse case: EPPE

In the EPPE, the first pulse is still of short duration and the second pulse is extended to satisfy Γ (or Γ_{ph})$T_{p2}\gtrsim 1$ and $kuT_{p2}\gg 1$ (but $\gamma_2 T_{p2}<1$). The notation is changed slightly to $\rho_1=\rho_{11}$, $\rho_2=\rho_{22}$, $\rho_3=\rho_{12}$, $\rho_4=\rho_{21}$. We write the time-dependent density-matrix elements as

$$\rho_n(v,t)=\sum_{m=1}^{4}\int G_{nm}(v,v',t-t_0)\rho_m(v',t_0)dv' ,$$
$$n=1,2,3,4 , \tag{3.7}$$

where the $G_{nm}(v,v',t-t_0)$ are elements of a propagator matrix satisfying the initial condition

$$G_{nm}(v,v',0)=\delta(v-v')\delta_{nm}, \quad n,m=1,2,3,4 . \tag{3.8}$$

Since the time evolution of the density matrix obeys a linear differential equation with constant coefficients, the time variable in the propagator G can be written as a time difference $t-t_0$.

Generally, by substituting Eq. (3.7) into the QMTE (3.3), one can get the corresponding time-evolution equation for the propagators G_{nm}. In order to solve the echo problem, we write the equation in the four time intervals (to be defined below) and solve for the propagators in each interval. Basically, the relevant density-matrix elements and the corresponding propagator elements in four intervals contributing to the echo may be expressed schematically as

$$\rho_1(v,t_0)\xrightarrow{G_{31}^{I}}\rho_3(v_1,t_1)\xrightarrow{G_{33}^{II}}\rho_3(v_2,t_2)\xrightarrow{G_{43}^{III}}\rho_4(v_3,t_3)\xrightarrow{G_{44}^{IV}}\rho_4(v_4,t_e) , \tag{3.9}$$

where the superscripts (I,II,III,IV) of G indicate the four relevant time intervals. Thus, the final state ρ_4 can be expressed in terms of the product of propagators in each interval and the initial state density matrix as

$$\rho_4(t_e)=\int G_{44}^{IV}(v_4,v_3,t_e-t_3)G_{43}^{III}(v_3,v_2,t_3-t_2)G_{33}^{II}(v_2,v_1,t_2-t_1)G_{31}^{I}(v_1,v,t_1-t_0)\rho_{11}(v,0)dv_4dv_3dv_2dv_1dv . \tag{3.10}$$

The time-evolution equations for the propagators and the solutions in the four time intervals are discussed below.

I. $0<t<t_1$. In the first time interval, both velocity-changing collisions and Doppler-phase factors can be neglected. Since the initial condition is

$$\rho_n(v,0)=\begin{cases}w_0(v), & n=1\\ 0, & n=2,3,4\end{cases} \tag{3.11}$$

it is an easy matter to show that, to first order in the field,

$$G_{31}^{I}(v_1,v,t_1)\approx -i\chi_1 t_1\delta(v-v_1) \tag{3.12}$$

provides that $kut_1\ll 1$.

II. $t_1<t<t_2$. In the second time interval, the field is absent and collisions play a role. Substituting Eq. (3.7) into Eq. (3.3) and setting $\chi=0$, one finds that, in this interval, only diagonal terms of the propagator matrix contribute since there is no coupling by the field. The diagonal propagator elements then satisfy

$$\frac{\partial G_{11}^{II}(v,v',\tau)}{\partial\tau}=-\Gamma G_{11}^{II}(v,v',\tau)+\int w(v''-v)G_{11}^{II}(v'',v',\tau)dv'' , \tag{3.13a}$$

$$G_{22}^{II}=G_{11}^{II} , \tag{3.13b}$$

$$\frac{\partial G_{33}^{II}(v,v',\tau)}{\partial\tau}=-(\Gamma+\Gamma_{ph}-ikv)G_{33}^{II}(v,v',\tau)+\int w(v''-v)G_{33}^{II}(v'',v',\tau)dv'' , \tag{3.13c}$$

$$\frac{\partial G_{44}^{II}(v,v',\tau)}{\partial\tau}=-(\Gamma+\Gamma_{ph}+ikv)G_{44}^{II}(v,v',\tau)+\int w(v''-v)G_{44}^{II}(v'',v',\tau)dv'' . \tag{3.13d}$$

By using Fourier transform techniques, one can write out the solution explicitly as

$$G_{11}^{II}(v,v',\tau)=\frac{1}{2\pi}\int_{-\infty}^{\infty}e^{-ik(v-v')t}e^{-\Omega_{11}(t)\tau}dt , \tag{3.14a}$$

$$G_{33}^{II}(v,v',\tau)=\frac{e^{ikv_2\tau}}{2\pi}\int_{-\infty}^{\infty}e^{ik(v-v')t}e^{-\Omega_{33}(t)\tau}dt , \tag{3.14b}$$

$$G_{44}^{II}(v,v',\tau)=\frac{e^{-ikv_2\tau}}{2\pi}\int_{-\infty}^{\infty}e^{ik(v-v')t}e^{-\Omega_{44}(t)\tau}dt , \tag{3.14c}$$

where

$$\Theta_{11}(t) = \Gamma \int_{-\infty}^{\infty} w(x) e^{-ikvt} dx = \Gamma(1 - e^{-k\sigma t/2^{1/2}}) , \tag{3.15a}$$

$$\Theta_{33}(t,\tau) = \Gamma + \Gamma_{ph} - \int_{-\infty}^{\infty} \int_{0}^{t} \frac{w(x)}{\Gamma} e^{ikv(t+\tau)} d\tau dx = \Gamma_{ph} + \Gamma \left| 1 - \frac{1}{\Gamma} \int_{0}^{t} \exp\{-[k\sigma(t+\tau')/2]^2\} d\tau' \right| , \tag{3.15b}$$

$$\Theta_{44}(t,\tau) = \Gamma + \Gamma_{ph} - \int_{-\infty}^{\infty} \int_{0}^{t} \frac{w(x)}{\Gamma} e^{ikv(t-\tau)} d\tau dx = \Gamma_{ph} + \Gamma \left| 1 - \frac{1}{\Gamma} \int_{0}^{t} \exp\{-[k\sigma(t-\tau')/2]^2\} d\tau' \right| . \tag{3.15c}$$

According to the echo formation sequence (3.9), G_{33}^{II} is the propagator of interest in the second time interval.

III. $t_2 < t < t_3$. In the third time interval, both collisions and the laser field influence the evolution of the density matrix. To find the propagator in this interval, it is more convenient to write Eq. (3.3) in vector notation as

$$\dot{\boldsymbol{\rho}}(v,t) = (\mathbf{D} + \mathbf{B})\boldsymbol{\rho}(v,t) + \int w(v'-v)\boldsymbol{\rho}(v',t)dv' , \tag{3.16}$$

where $\mathbf{D}$ is a diagonal matrix given by

$$\mathbf{D} = \begin{vmatrix} \Gamma & 0 & 0 & 0 \\ 0 & \Gamma & 0 & 0 \\ 0 & 0 & (\Gamma + \Gamma_{ph} - ikv) & 0 \\ 0 & 0 & 0 & -(\Gamma + \Gamma_{ph} + ikv) \end{vmatrix} \tag{3.17}$$

and $\mathbf{B}$ is a field coupling matrix given by

$$\mathbf{B} = i \begin{vmatrix} 0 & 0 & \chi & \chi \\ 0 & 0 & \chi & -\chi \\ \chi & \chi & 0 & 0 \\ \chi & -\chi & 0 & 0 \end{vmatrix} . \tag{3.18}$$

A formal solution to Eq. (3.3), written as an iterative expression in terms of the field-free propagators, is given by[24]

$$\rho_n(v,t) = \sum_m \int G_{nm}^{II}(v,v',t-t_0)\rho_m(v,t_0)dv' + \sum_{l,m} \int dv' \int_{t_2}^{t} dt' G_{nm}^{II}(v,v',t-t') \times B_{ml}\rho_l(v',t') , \tag{3.19}$$

where the G_{nm}^{II} are the field-free propagators already calculated for region II. Substituting Eq. (3.7) into Eq. (3.19), one finds a corresponding iterative expression of the matrix propagator in the third interval as

$$G_{nm}^{III}(v,v',\tau) = G_{nm}^{II}(v,v',\tau) + \int dv'' \int_{0}^{\tau} d\tau' \sum_{k,l} G_{nk}^{II}(v,v'',\tau-\tau')B_{kl}G_{lm}^{III}(v'',v',\tau') . \tag{3.20}$$

Since $\chi T_{p2} \ll 1$, the perturbation-theory limit is applicable and Eq. (3.20) can be solved to second order in the field strength. The element G_{43} contributing to echo formations is given by

$$G_{43}^{III}(v_3,v_2,t_3-t_2) = 2\chi_2^2 \int_{-\infty}^{\infty} dv'' dv' \int_{t_2}^{t_3} \int_{t_2}^{t'} dt'' dt' G_{44}^{II}(v_3,v',t_3-t')G_{11}^{II}(v',v'',t'-t'')G_{33}^{II}(v'',v_2,t''-t_2) . \tag{3.21}$$

By carrying out some of the integrations, one obtains

$$\begin{aligned} G_{43}^{III}(v_3,v_2,t_3-t_2) = 2\chi^2 \int_{t_2}^{t_3} \int_{t_2}^{t'} dt'' dt' dt \exp[-ikv_3(t_3-t'-t) + ikv_2(t''-t_2-t)] \\ \times \exp[-\Theta_{44}(t,t_3-t')(t_3-t') - \Theta_{33}(t-t''+T_2,t''-t_2)(t''-t)] \\ \times \exp[-\Theta_{11}(t)(t'-t'')] . \end{aligned} \tag{3.22}$$

IV. $t_3 < t < t_4$. In the fourth interval the field is again absent and collisions play a role. The calculational procedure is the same as in the second interval, but the propagator element of interest in this interval is $G_{44}^{IV} = G_{44}^{II}$, given by Eq. (3.14c).

By substituting the propagators obtained for the four intervals into Eq. (3.10) and integrating over all velocity components at the echo time $t_4 = t_3 + t_2 - t_1$, one arrives at

$$\rho_3(t_4) = \frac{4iN}{ku} \pi\chi_1\chi_2^2 I_{p1} \int_{t_3}^{t_4} \int_{t_2}^{t'} dt'' dt' e^{-\Theta_{44}(t_4-t')(t_4-t')} e^{-\Theta_{33}(t'-t''+T_2,t''-t_2)(t'-t'')} e^{-\Theta_{44}(t_4-t_3+t'-t'',t_3-t_2)(t_3-t_2)} \delta(t_4-t'-t'') , \tag{3.23}$$

where use has been made of the relations

$$\Theta_{33}(x_1,x_3-x_1)(x_3-x_1) = \Theta_{33}(x_1,x_2-x_1)(x_2-x_1) + \Theta_{33}(x_2,x_3-x_2)(x_3-x_2) , \tag{3.24a}$$

$$\Theta_{33}(x_1,x_4-x_2)(x_4-x_2) = \Theta_{44}(x_1,x_3-x_2)(x_3-x_2) + \Theta_{44}(x_4-x_3,x_4-x_3), \quad x_4 > x_3 > x_2 > x_1 . \tag{3.24b}$$

The relaxation properties of the echo signal are characterized by three Θ functions defined for time intervals $0 \rightarrow t''$, $t'' \rightarrow t'$, and $t' \rightarrow t_e$. Before carrying out the time integrations, we give a physical interpretation of each Θ function.

The quantity $\Theta_{33}(0,t'')$ represents a modified decay rate of coherence density, owing to velocity-changing collisions, in the time period $0 < t < t''$. The presence of the factor $\Theta_{33}(0,t'')$ in Eq. (3.23) reflects the fact that the dipoles continuously dephase up to time t'' when the second field switches them to population. Collisions occurring at times $t_{\rm coll}$ $(0 < t_{\rm coll} < t'')$ induce the phase shifts, giving rise to an average decay rate $\Theta_{33}(0,t'')$. All possible switching times t'' from t_2 to t_3 must be allowed.

The quantity $\Theta_{11}(t'')$, as defined by Eq. (3.15a), represents the decay rate of population density after time t''. Since no additional dephasing occurs after t'', the magnitude of Θ_{11} depends critically on the previous net phase kvt'' of atoms which have not undergone collisions. If kvt'' is small, Θ_{11} is small regardless of the number of collisions occurring between t_2 and t_3. The major contribution to the echo signal occurs as t'' approaches t_2, for which kvt'' is minimum. The time period for which the signal decays at rate $\Theta_{11}(t'')$ is determined by the second switching time that transfers the population back to coherence. If the second switching time is denoted by t', then the signal decays at rate $\Theta_{11}(t'')$ from t'' to t'. The times t'' and t' both vary from t_2 to t_3 with $t' > t''$. An appropriate average over all t'' and t' is necessary.

In the third interval, the decay rate of coherence density is $\Theta_{44}(t'', t_e - t')$. The previous net phase of atoms undergoing no collisions is still kvt'' preserved through the period $t' - t''$. The interval $t_3 - t'$ is a rephasing period in which the additional phase produced has an opposite sign to that from the first interval. In this case, the net phase to be affected by collisions is the difference of the previous phase and the phase produced in the interval $t_e - t'$.

One may conclude from this discussion that the three Θ functions exhibit very clearly the collision-induced relaxation of the echo signal in the three time intervals. In the first and third intervals, the Θ_{33} and Θ_{44} represent the decay rate of coherence density. The effect of collisions on the Doppler-phase factor depends on the previous net phase plus additional phase in these two intervals. In the second interval, Θ_{11} represents the decay rate of population density. The collision effect depends only on the previous net phase and the number of collisions. If the previous phase is sufficiently small such that the phase shift is less than unity, the collision-induced decay is, in effect, suspended in the second time interval. The relationship of this theoretical result to the experiment of Yodh *et al.*[19] is discussed below.

It should be noticed that the symmetry property indicated by the δ function in Eq. (3.23) is the same as that for EPPE result without velocity-changing collisions. As a result of collisions, however, the number of symmetric pulse strips that contribute to the echo is reduced. The new region of symmetric pulse strips that contribute can be found by solving Eq. (3.23). By performing the time integration over t'' in Eq. (3.23), one can get a simpler expression of the form

$$\rho_4(t_e) = -\frac{4i\sqrt{\pi}\chi_1\chi_2^2 T_{p1}}{ku} e^{-(\Gamma+\Gamma_{\rm ph})t_e} \int_0^{T_{p2}/2} dt\, e^{2\Gamma\sqrt{\pi}/k\sigma\,\mathrm{erf}[(k\sigma/2)(t_2+t)]} \times \exp\{\Gamma(T_{p2}-2t)\exp\{-[k\sigma(t_2+t)/2]^2\} + \Gamma_{\rm ph}(T_{p2}-2t)\} . \quad (3.25)$$

By expanding the integrand, one finds an effective coherence time (that is, the maximum time t for which the integrand is non-negligible)

$$t_{\rm eff} \approx \frac{1}{k\sigma\sqrt{\Gamma T_{p2}}} . \quad (3.26)$$

The quantity $t_{\rm eff}$ represents the effective time of the atom-field interaction in the second pulse interval. For example, if t_2 and t_3 are fixed, this long-pulse echo sequence can be described as a quasistimulated echo scheme in which the "second pulse" starts at t_2 and has a duration $t_{\rm eff}$ while the "third pulse" starts at $t_3 - t_{\rm eff}$ and also has a duration $t_{\rm eff}$. The effective pulses can, in turn, be divided into pulse strips of short duration, so that the signal can be viewed as arising from a short-pulse duration stimulated echo, with the second and third pulses provided by these symmetric strip pairs. One can conclude that, for no collisions, the major contribution to the echo is from all symmetric pulse pairs in the entire region of pulse 2; with velocity-changing collisions, the major contribution to the echo is from those symmetric pulse pairs within a coherence time $t_{\rm eff}$ of the pulse borders of the second pulse region (see Fig. 12). Therefore, the use of an extended pulse in a two-pulse excitation scheme is inefficient when collisions are present, since the central part of the second pulse does not contribute to the echo formation.

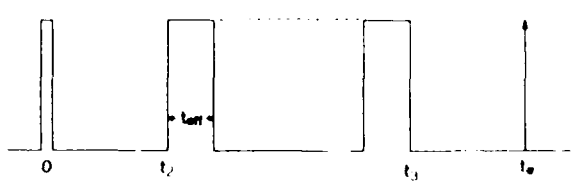

FIG. 12. In the presence of collisions, the extended-pulse photon echo can be described equivalently as a stimulated photon echo with the second and third pulse's durations defined by an effective coherence time $t_{\rm eff}$. Note that as a result of collisions, symmetric pairs of pulses from the central region of the excitation pulse (see Fig. 7) no longer contribute to echo formation.

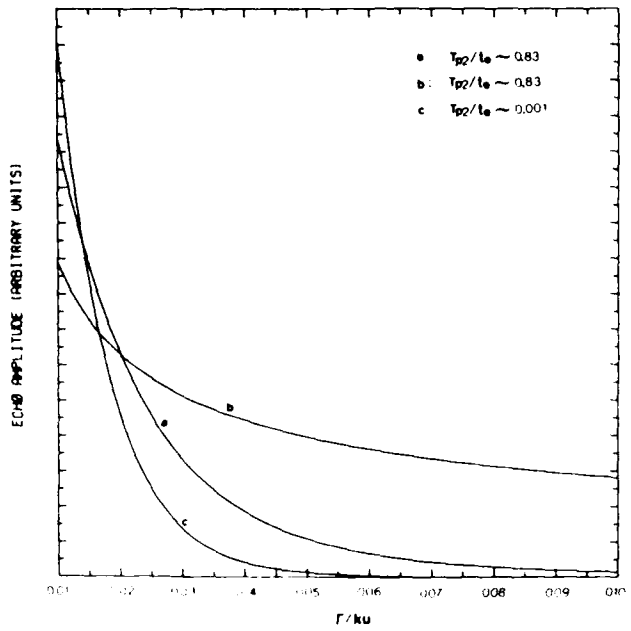

FIG. 13. Variation of the echo amplitude (arbitrary units) with pressure (in units of Γ/ku). Curves (*a*) and (*b*) represent solution for EPPE in which $T_{p2}/t_e \sim 1$. Curve (*a*) is a numerical solution to Eq. (3.25) and curve (*b*) is an approximate analytic solution of Eq. (3.25) which varies as $(\Gamma T_{p2})^{-1/2}$. For reference purposes, curve (c) is plotted in the limit that $T_{p2}/t_e \ll 1$. In this case, the signal decays exponentially as $\exp(-\Gamma t_e)$.

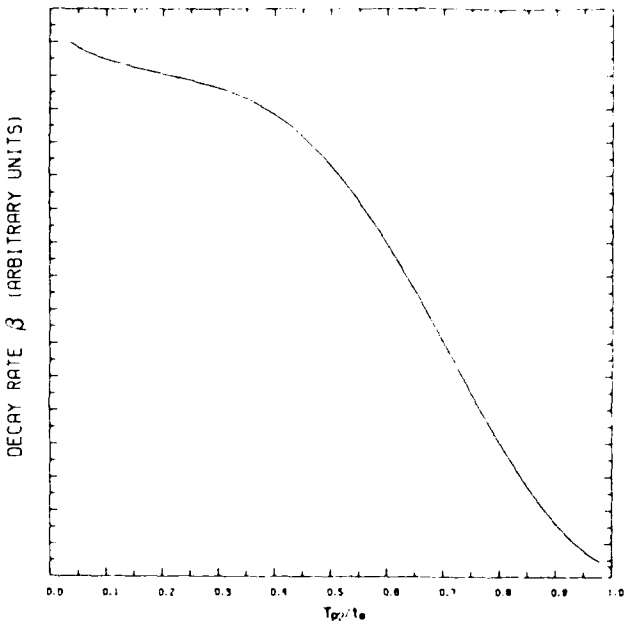

FIG. 14. Variations of the echo decay rate [β, defined by Eq. (3.28)] of the photon echo with the second pulse's duration (T_{p2}) for the weak-field limit. In this figure, the parameters are chosen as $\Gamma_{ph}=0$, $\Gamma/ku=0.5$, and $\sigma/u=0.06$.

It is interesting to compare variations of echo amplitude as a function of the collision rate for the short- and extended-pulse photon echoes. One can see from Fig. 13 that, for short-duration pulses, the signal decays exponentially with increasing collision rate Γ [curve (c)]. For an extended pulse (for example, $T_{p2}/t_e \approx 0.83$), the signal dependence on Γ is shown in curve (a) of Fig. 13. To find an approximate analytical expression characterizing curve (a), we expand Eq. (3.25) to get

$$\rho_4(t_e) \sim \frac{1}{k\sigma\sqrt{\Gamma T_{p2}}} \tag{3.27}$$

which is plotted as curve (b). The variations of curves (a) and (b) are very similar, which illustrates that the dependence of echo amplitude on the velocity-changing collision rate changes from $\exp(-\Gamma t_e)$ for $T_{p2} \ll t_e$ to $(\Gamma T_{p2})^{-1/2}$ for $T_{p2} \sim t_e$.

The analysis of the EPPE in the time and frequency domains allows us to understand the increase in echo signal with increased duration of the second pulse. First, regardless of velocity-changing collisions, it is always true that the longer the second pulse, the larger the population difference created (recall that there is no saturation on the echo amplitude as a function of the second pulse's duration in this perturbative treatment). Consequently more dipoles are stimulated to emit with longer second pulses, as has been discussed in Sec. II. Second, as the second pulse's duration is extended, there is a larger time range when population density rather than coherence density exists during the pulse. In order words the pulse sequence acts as a stimulated photon echo with the second and third effective pulses formed from the beginning and end of the long excitation pulse. Therefore, if the phase buildup before pulse 2 is sufficiently small, the decay due to velocity-changing collisions is mostly suppressed during pulse 2, as in the stimulated photon echo. As a result the echo increases and decay rate decreases relative to that of the two-pulse echo.

The above features may be seen in the curve of Fig. 14, which plots the echo decay rate β as a function of T_{p2}, where β is defined as

$$I_e = I_0|\rho_4(t_e)| \sim e^{-\beta(T_{p2}/P)} \tag{3.28}$$

in which P is the perturber pressure. Figure 14 represents a numerical solution of Eq. (3.25), in which $\Gamma_{ph}=0$, $\Gamma/ku=0.5$, and $\sigma/u=0.06$. As long as $k\sigma t_2 \gg 1$ (that is, for relatively short T_{p2}), the echo decay rate as a function of T_{p2} is approximately constant. There is no suppression of decay in the "population zone" which occurs during pulse 2, since the phase buildup before this zone is sufficiently large to guarantee that any collision during the population zone kills the echo signal. As T_{p2} increases, t_2 becomes relatively smaller such that $k\sigma t_2 < < 1$. In that case, collisions during the population zone do not diminish the echo amplitude and the echo amplitude grows dramatically with increasing T_{p2}. This result exhibits a feature that is essentially similar to an experimental phenomenon observed by Yodh *et al.* in an extended-pulse photon echo,[19] even though the physical parameters in the experiment are not consistent with either the weak-field theory of this paper or the value of Γ/ku used in plotting Fig. 14. In a planned

companion paper for strong fields, we will give a detailed discussion and comparison between the theory and the experiment for the appropriate physical parameters. At this point, however, we can note that a decrease in decay rate for the EPPE is already seen in the weak-field limit and, provided that $\gamma/ku \ll 1$, does not appear to be directly connected with a "strong-field quenching", as has been previously proposed.[19] Instead, it will be shown that the mechanism responsible for the decrease in the decay rate is the same as that already appearing in the weak-field theory.

ACKNOWLEDGMENTS

This research was supported by the National Science Foundation under Grant No. PHY 8415781 and by the U.S. Office of Naval Research.

*Present address: Department of Physics, Beloit College, Beloit, WI 53511.

[1]I. D. Abella, N. A. Kurnit, and S. R. Hartmann, Phys. Rev. **141**, 391 (1966).

[2]P. R. Berman, *Advances in Atomic and Molecular Physics*, (Academic, New York, 1977), Vol. 13, p. 57, and references therein.

[3]P. R. Berman, J. M. Levy, and R. G. Brewer, Phys. Rev. A **11**, 1668 (1975).

[4]A. Flusberg, T. Mossberg, and S. R. Hartmann, Opt. Commun. **24**, 707 (1978).

[5]A. Flusberg, Opt. Commun. **29**, 123 (1979).

[6]R. A. Forber, L. Spinelli, J. E. Thomas, and M. S. Feld, Phys. Rev Lett. **50**, 331 (1983).

[7]J. E. Thomas, R. A. Forber, L. A. Spinelli, and M. S. Feld, Phys. Rev. Lett. **51**, 2194 (1983).

[8]T. W. Mossberg, R. Kachru, and S. R. Hartmann, Phys. Rev. Lett. **44**, 73 (1980).

[9]A. Flusberg, Opt. Commun. **29**, 123 (1979).

[10]R. A. Forber, L. Spinelli, J. E. Thomas, and M. S. Feld, Phys. Rev. Lett. **50**, 331 (1983).

[11]K. P. Leung, T. W. Mossberg, and S. R. Hartmann, Phys. Rev. A **26**, 3097 (1982).

[12]P. R. Berman and W. E. Lamb, Phys. Rev. A **2**, 2435 (1970).

[13]P. R. Berman and W. E. Lamb, Phys. Rev. A **4**, 319 (1971).

[14]P. R. Berman, Phys. Rev. A **5**, 927 (1972).

[15]P. R. Berman, Phys. Rep. **43**, 101 (1978).

[16]P. R. Berman, *New Trends in Atomic Physics* (North-Holland, Amsterdam, 1984), p. 453.

[17]P. R. Berman, Appl. Phys. (Germany) **6**, 283 (1975).

[18]P. R. Berman, J. Opt. Soc. Am. B **3**, 564 (1986).

[19]A. G. Yodh, J. Golub, and T. W. Mossberg, Phys. Rev. Lett. **53**, 659 91984).

[20]R. Shoemaker, *Laser and Coherence Spectroscopy*, edited by J. T. Steinfeld (Plenum, New York, 1978), p. 197.

[21]The dependence of the echo signal on $\Gamma_{p1}T_{p2}$ has been studied by Durrant and Manners [A. V. Durrant and J. Manners, Opt. Acta **31**, 1167 (1984)]. In their calculation, they assumed $kuT_{p2} \ll 1$, which is not consistent with our assumption that $kuT_{p2} \gg 1$ for an EPPE; consequently, the two theories cannot be compared directly. Experimentally (Yodh *et al.*, Ref. 19), $kuT_{p2} \approx 1000$. In any event, it is argued in our companion paper that homogeneous broadening alone cannot provide a consistent explanation of the data.

[22]N. G. Van Kampen, *Stochastic Processes in Physics and Chemistry* (North-Holland, Amsterdam, 1981).

[23]G. E. Uhlenbeck and L. S. Ornstein, Phys. Rev. **36**, 823 (1930).

[24]P. R. Berman, J. Opt. Soc. Am. B **3**, 572 (1986), and references therein.